Search for WIMP Inelastic Scattering Off Xenon Nuclei With Xenon100 Data*

Ann Author† and Second Author‡
Authors' institution and/or address
*This line break forced with *
(XENON Collaboration)

Authors
Second institution and/or address
This line break forced and
Affiliation
(Dated: January 5, 2017)

I. INTRODUCTION

Astrophysical evidence indicates that the dominant mass fraction of our Universe consists of some yet unknown form of dark matter. Well motivated models predict Dark Matter in the form of Weakly Interacting Massive Particles (WIMPs), hypothesis which is currently being tested by several direct and indirect detection experiment.

Most of direct detection searches focuses on elastic scattering of dark matter particles off nuclei. In this analysis instead we explore an inelastic scattering process, we consider the ^{129}Xe isotope being excited to a low-lying state with subsequent prompt de-excitation via the emission a photon. This isotope is an excellent target since its abundance in natural xenon is of 26.4% and a relatively low energy is necessary to excite its 3/2+ state above the 1/2+ spin ground state. Inelastic WIMP-nucleus scattering in xenon is complementary to elastic scattering for spin-dependent interactions, the former dominates the integrated rate above $\simeq$ 10 keV of energy deposition. Furthermore, in the case of dark matter detection, this channel can be employed to asses whether the nature of the fundamental interaction is spin-dependent or not.

II. XENON100 DETECTOR

The Xenon100 experiment is a dual phase liquid xenon TPC. For a given interaction in the liquid target this type of detector produces two separated signals, one proportional to the prompt scintillation (S1) the other to ionization (S2).

To add: sentences about detector stability, science run data used, Ly and Y measurements used.

III. DATA ANALYSIS

This analysis is performed using XENON100 Run-II science data, which corresponds to 224.9 live days. The detector response to electronic recoil (ER) has been characterized using ^{60}Co and ^{232}Th radioactive sources, while response to inelastic nuclear recoil (NR) scattering was calibrated using an ^{241}AmBe source.

The inelastic scattering of a WIMP with the nucleus of ^{129}Xe produces an energy deposit via nuclear recoil with subsequent emission of a 39.6 KeV de-exitation photon. The largest fraction of the energy released in the event is via electronic recoil (ER) due to the emitted photon, this represents an unusual signature for this kind of detector and brings the signal to overlay a phase space region with large backgrounds. The choosen region of interest for this analysis surrounds the 39.6 KeV line in the cS1-cS2 plane which is further divided into sub regions, as shown in figure 1.

Events are asked, other than falling in the defined region of interest, to fullfill several selection criteria: quality selection aimed to reduce noise impact toghether with energy and threshold selection on S2, selection of single scatter events and fiducial volume definitions are reported in detail in [6], this analysis follows the selection reported there for Run-II, only few modification have been designed specifically for this analysis and discussed below. In particular, selection on S2 width as a function of drift time has been optimized on a sample of events from 40 KeV of AmBe and set to a 95% acceptance on those type of events. Events are required to be single scatter by applying a threshold on the second largest S2 peak size, in this analysis the threshold has been set to 160 PE and constant in S2 signal size. The fiducial volume chosen for this analysis corresponds to 34 Kg of liquid xenon.

A. Signal Simulation

The detector response to inelastic scattering of WIMPs of different masses off ^{129}Xe nucleus was simulated using an empirical model. The total deposited energy is divided into two independent contributions: the one re-

*
† Also at Physics Department, XYZ University.
‡ Second.Author@institution.edu

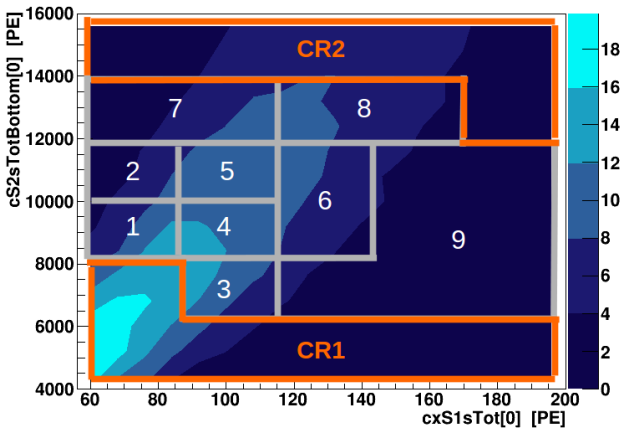

FIG. 1. Signal region and control region.

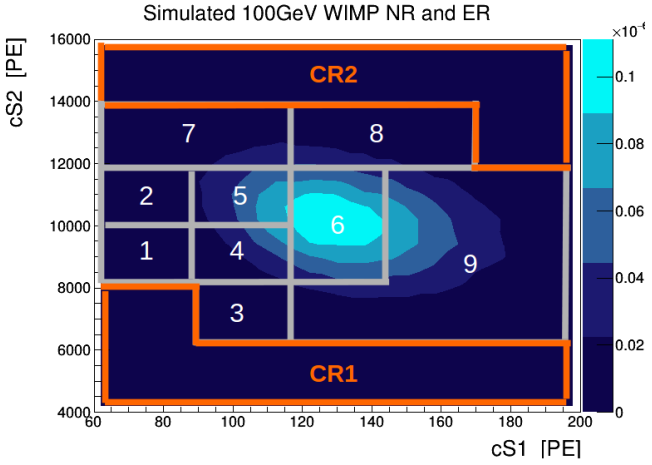

FIG. 2. Signal region and control region, for WIMP of mass 100 GeV.

lated to the 39.6 KeV de-exitation photon and the one relative to the simultaneous nuclear recoil (NR) of the Xe atom, the number of photons and charge yield detected is simulated separatedly for each contribution and then added togheter.

The electronic recoil (ER) induced by the de-exitation photon is produced The detector related light yield L_y measured at 39.6 KeV with AmBe calibration has been found to have a large systematic uncertainty due to the contribution of the nuclear recoil, so the light yield used to describe the number of photon detected is the result of a fit to data, corresponding to several lines, of the NEST model [1, 2, 11]. The same model is used predict the charge yield at 39.6 KeV whichis then scaled according to the detector's secondary scintillation factor Y, determined from detector response to single electrons [9], note that the corrected S2 observed by the bottom PMT array is used in this analysis. This is how the average μ_{cS1} and μ_{cS2} are obtained. The detector resolution at 39.6 KeV is embedded in three parameter the standard deviation in cS1 and cS2, respectively σ_{cs1} and σ_{cs2} and the correlation, ρ, between cS1 and cS2. The correlation parameter is assumed to be independent of energy (at least in the considered range) and measured using the 164 KeV Xenon activated line by AmBe calibration source, this line is choosen since allows to disentangle efficiently contribution from nuclear recoil, the measured correlation is $\rho = -0.45 \pm 0.10$. Finally a two dimensional normal distribution, which is depicted in formula 1 except a normalization factor, is employed as a probability density function $f(cS1, cS2)$ distribution of energy deposited from the 39.6 KeV photon.

$$f(cS1, cS2) = exp\Big(- \frac{1}{2(1-\rho^2)} \Big[\frac{(cS1-\mu_{cS1})^2}{\sigma_{cs1}^2} + \frac{(cS2-\mu_{cS2})^2}{\sigma_{cs2}^2} - \frac{2\rho(cS1-\mu_{cs1})(cS2-\mu_{cs2})}{\sigma_{cs1}\sigma_{cs2}} \Big] \Big) \quad (1)$$

The cS1 and cS2 distributions from NR contribution to the total signal are predicted starting from the nuclear recoil energy spectrum for inelastic interaction of a given WIMP mass [7], the average cS1 and cS2 are given by formula 2 and 3 respectively, where $\mathcal{L}_{eff}$ is the LXe relative scintillation efficiency while $S_{ee} = 0.58$ and $S_{nr} = 0.95$ describe the scintillation quenching due to the electric field [3]. The parameterization and uncertainties of $\mathcal{L}_{eff}$ as a function of E_{nr} are based on existing direct measurements [4]. The light yield at 122 keVee originate from the same NEST model fit as described above. For the cS2 the parameterization of $Q_Y(E_{nr})$ is taken from [5]. all detector related resolution effects are introduced following the prescriptions described in [6].

$$cS1_{nr} = E_{nr}\, \mathcal{L}_{eff}(E_{nr})\, L_Y\, \frac{S_{nr}}{S_{ee}} \quad (2)$$

$$cS2_{nr} = E_{nr}\, Q_Y(E_{nr})\, Y \quad (3)$$

The pdf of the ER and NR contributions are then convoluted toghether to obtain the overall pdf of the signal. A 2D (cS1 versus cS2) acceptance map is applied to the signal pdf to reproduce data selection effects, single selection acceptances are computed using calibration samples of AmBe for all the selection criteria except the outer volume veto and the single interaction selections, for which a detailed computation has been performed. The average acceptance value in the region of interest is of about 0.80 ± 0.05. An example of signal model is in Figure 1 for a WIMP of 100 GeV. The simulation of the 39.6 KeV line has been compared to AmBe data, for the comparison the proper AmBe nuclear recoil and acceptances were simulated, the model was found in very well in agreement with calibration source data showing the largest discrepancies within statistical uncertainties.

B. Background Model

The expected background in the region of interest is mainly caused by material radioactivity, mainly photons that interact via compton scattering, background due to activation of Xe 39.6 line from radiogenic neutrons is found to be negligible. To model this background we use data from ^{60}Co calibration campaign, the assumption is that the ^{60}Co data are representative of the density in cS1-cS2 plane of the background. The calibration sample events in the ROI amount to 22225 events, this yield is then scaled to data according to a measured background scale factor τ_{bkg}.

The scale factor is measured in the two control regions shown in Figure 1 and labelled CR1 and CR2, the two control regions give compatible results and the computed average is $\tau_{bkg} = 0.034 \pm 0.002$, where the reported uncertainty is of statistical nature only.

The distribution of the calibration sample has been compared to the data of the sience run in the two control regions, agreement is found within statistical uncertainties. ^{60}Co calibration data have been compared in the region of interest to data from ^{232}Th calibration campaign, the largest deviation between the two shapes is within 4%. An additional systematic uncertainty of 4% has been applied to the expected background yield of each subregion of the ROI.

C. Systematic Uncertainties

Uncertainties on the total prediction of background events arise from the relative uncertainties on the measure of the normalization factor τ_{bkg} and amount to 6%, while uncertainties arising from radiogenic neutrons contributions are neglected. Uncretainty on the shape of the predicted bakground distribution are assesed by reporting the maximal discrepancy in the ROI between the ^{60}Co and ^{232}Th calibration samples, according to this it is assigned to the expected yield of each subregion a 4% uncertainty, uncertainty belonging to different regions are considered independent from each other.

Signal model, Energy scale uncertainties.... Uncertainties related to energy scale and more generally to detector response are taken into account by relative uncertainties on the measure of L_Y,$\mathcal{L}_{eff}$,Y, Q_Y and ρ. Has been shown by the simulation that these type of uncertainty affect the total signal yield in the ROI by less than a percent for a wide range of masses, however they greatly affects the pdf of the signal model in the ROI. For each WIMP mass several signal simulation sample are produced warying these parameter respectively $\pm 1\sigma$, for each region is computed an uncertainty by adding in quadrature the variations with respect to nominal of each case, Figure 3 is an example of such a systematic uncertainty computation for WIMP mass of 100 GeV.

Uncertainty on the total yield of the signal arising from uncertainties on the selection acceptance are found to be very weakly dependent on the WIMP mass, an overall 6% acceptance uncertainty is then applied to all WIMP hypotesis.

All the uncertainties discussed here are threated as nuissance parameter in the likelihood, which are contrained by a gaussian distribution.

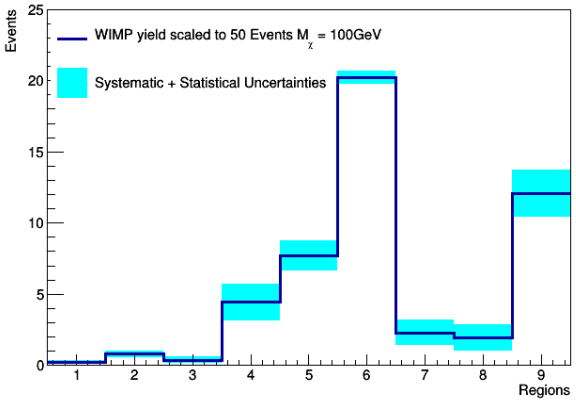

FIG. 3. Signal region, uncertainties for WIMP of mass 100 GeV.

IV. RESULTS

In an exposure of 34 Kg per 224 days of liquid xenon a yield of 764 events are found in the region of interest, which is compatible with the expectation of $756 \pm 5^{(stat.)} \pm 55^{(syst.)}$. The distribution of events from data are compared to the background expectation in Figure 4 and with the relative uncertainties. This result is interpreted via a binned profiled likelihood approach by means of the test statistic $\tilde{q}$ and its asymptotic distributions described in [8]. 90% CL$_s$ [10] confidence level limits are computed on the spin dependent cross section as a function of the WIMP mass and shown in Figure 5.

[1] S. Agostinelli et al. GEANT4: A Simulation toolkit. *Nucl. Instrum. Meth.*, A506:250–303, 2003.

[2] John Allison et al. Geant4 developments and applications. *IEEE Trans. Nucl. Sci.*, 53:270, 2006.

[3] E. Aprile, C. E. Dahl, L. DeViveiros, R. Gaitskell, K. L. Giboni, J. Kwong, P. Majewski, Kaixuan Ni, T. Shutt, and M. Yamashita. Simultaneous measurement of ionization and scintillation from nuclear recoils in liquid xenon

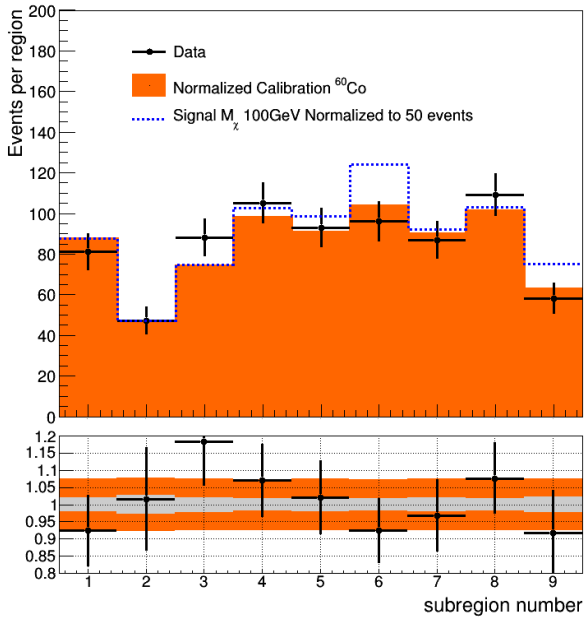

FIG. 4. Results, comparison between data and expected background.

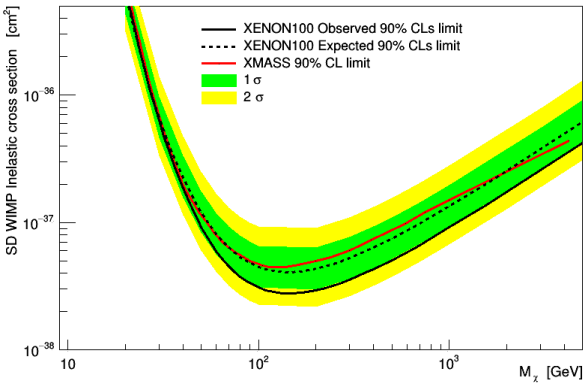

FIG. 5. Observed and expected limits.

as target for a dark matter experiment. *Phys. Rev. Lett.*, 97:081302, 2006.

[4] E. Aprile et al. Dark Matter Results from 100 Live Days of XENON100 Data. *Phys. Rev. Lett.*, 107:131302, 2011.

[5] E. Aprile et al. Response of the XENON100 Dark Matter Detector to Nuclear Recoils. *Phys. Rev.*, D88:012006, 2013.

[6] E. Aprile et al. XENON100 Dark Matter Results from a Combination of 477 Live Days. *Phys. Rev.*, D94(12):122001, 2016.

[7] L. Baudis, G. Kessler, P. Klos, R. F. Lang, J. Mendez, S. Reichard, and A. Schwenk. Signatures of Dark Matter Scattering Inelastically Off Nuclei. *Phys. Rev.*, D88(11):115014, 2013.

[8] Glen Cowan, Kyle Cranmer, Eilam Gross, and Ofer Vitells. Asymptotic formulae for likelihood-based tests of new physics. *Eur. Phys. J.*, C71:1554, 2011. [Erratum: Eur. Phys. J.C73,2501(2013)].

[9] E Aprile et al. Observation and applications of single-electron charge signals in the xenon100 experiment. *Journal of Physics G: Nuclear and Particle Physics*, 41(3):035201, 2014.

[10] Alexander L. Read. Modified frequentist analysis of search results (The CL(s) method). In *Workshop on confidence limits, CERN, Geneva, Switzerland, 17-18 Jan 2000: Proceedings*, pages 81–101, 2000.

[11] M Szydagis, A Fyhrie, D Thorngren, and M Tripathi. Enhancement of nest capabilities for simulating low-energy recoils in liquid xenon. *Journal of Instrumentation*, 8(10):C10003, 2013.